



The Effects of Building Glass Façade Geometry on Wind Infiltration and Heating and Cooling Energy Consumption

Amiraslan Darvish^{1*}, Seyed Rahman Eghbali¹, Golsa Eghbali², Yousef Gorji Mahlabani¹

¹*Department of Architecture and Urban Development, Imam Khomeini International University, Qazvin, Iran*

²*Department of Architecture Engineering, University of Zanjan, Zanjan, Iran*

Abstract. The control of energy loss through building envelopes has always been a passive design solution for architecture and improvements in space quality. A significant factor is the control of infiltration through the geometry of the glass façades of buildings. The uncontrolled input air flow from the outside into an interior space is known as infiltration. The main infiltration factor is the pressure difference between a building's interior and exterior. This difference might result from the interaction of the wind with the façade. Other possible causes are the stack effect and mechanical ventilation. There is a fundamental question about the effects of the outer glass shell geometry on wind infiltration and building energy consumption. The purpose of this study was to investigate the geometries of building façades with glass materials in different climates and to measure wind infiltration. Consequently, building energy simulations were performed to calculate the infiltration rates in building shells with different geometries. Four forms were simulated, and the effects of the wind infiltration-induced air exchange on heating and cooling energy consumption were evaluated in four climates in Iran. The results indicate that convex geometry reduces the wind pressure in the outer shell and the air exchange rate resulting from the infiltration; thus, heating and cooling energy consumption is reduced.

Keywords: Energy consumption; External geometry; Infiltration; Simulation; Wind pressure

1. Introduction

The building sector is responsible for approximately 40% of the world's total annual energy consumption (Omer, 2008). This situation has therefore raised the need for sustainable designs for reducing energy consumption in buildings (Pacheco et al., 2012; Russ et al., 2018; Yusuf et al., 2018). The sustainable development principles in the built environment have encouraged researchers to focus on more efficient building envelopes (Hong et al., 2019). A principal constituent of building envelopes, façades play a vital role in protecting indoor environments and controlling the interactions between outdoor and indoor spaces (Ghaffarianhoseini et al., 2016). Conventional façades can lead to poor natural ventilation, low daylight levels, thermal discomfort, and increased energy consumption (Yin et al., 2012; Luo et al., 2016). With the modern movement in architecture, vast glazed façades were introduced to improve the aesthetics of architecture. Now, many high-rise buildings around the world have fully glazed façades or large areas of glazing. Infiltration through glazed façades plays a significant role in energy loads and,

*Corresponding author's email: amiraslandarvish@gmail.com, Tel.: +98-936-2932336
doi: [10.14716/ijtech.v11i2.3201](https://doi.org/10.14716/ijtech.v11i2.3201)

consequently, energy demands and costs (Chen et al., 2012; Younes, et al., 2012).

Infiltration is unintended leakage, such as the flow of outdoor air through cracks in a building (ASHRAE, 1997). The main reason is the difference between the pressure inside the building and the pressure on its façade. This can be the result of wind pressure, the chimney effect, or mechanical ventilation (Jackman, 1974). Factors such as leakage, the quality of materials, the age of the building, the environmental conditions, and the geometry of the building have an effect on infiltration (Ji et al., 2005). Infiltration occurs through the building envelopes (Powell et al., 1989). It is a significant aspect in heat loss calculations, which play a fundamental role in determining the thermal load caused by the entry of outside air into a building. Air infiltration, along with ventilation, has a considerable effect on indoor environment quality. The moisture carried by infiltrating air leads to failures in the performance of building materials.

Airflow leakage also affects the distribution of indoor air pollutants and detrimental microbes (Lstiburek et al., 2002; Rantala and Leivo, 2009). Infiltration causes undesirable heating and ventilation conditions that lead to indoor overheating and excessive energy consumption (Liddament, 1986). In this context, it is possible to control the impact of the prevailing winds through the use of aerodynamic shells to minimize infiltration (Jokisalo et al., 2009). The static pressure at the outer surface of a building is produced by the interaction of the wind with the building shell, and this is influenced by wind speed and direction, air density, surface orientation, and environmental conditions. Depending on the wind angle and the building form, the pressure produced on the building exterior can be positive or negative, and this will influence the infiltration flow (Sherman, 1987). Thus, the building envelope would appear to have a significant influence on the infiltration factors. In this regard, buildings with glass façades are very important because of the direct interaction with outdoor environmental factors, such as sun radiation and wind velocity.

The purpose of this study was to investigate the wind-driven infiltration rate on the geometries of building façades and to determine the optimal forms for reducing energy consumption. In buildings with glass façades, the leakage rate is higher because of the unique type of envelope. Therefore, infiltration plays a significant role in reducing heating and cooling energy consumption. The study examined the effects of four forms (simple, indented, convex, and concave) on the infiltration rates on building façades in four climates in Iran. This facilitated energy simulation and modeling on the basis of the obtained data in order to determine the optimal forms for façades. Accordingly, the study has proposed optimal energy consumption solutions.

2. Research Background

Because of its importance, air infiltration has been measured and modeled in many studies. Most of these studies were conducted in the 1970s and 1980s when many measurement methods and computational models were introduced. Since then, studies have measured air infiltration in entire buildings or their components. Relander et al. (2008a, 2008b) conducted experiments to determine the effects of seal joints and openings on air leakage in buildings with fiberboard. This study of different types of buildings concluded that the building design process plays a significant role in infiltration. In an optimized building, air leakage was 24% lower than average; however, for a wood-frame building, it was 16% higher than average. Sfakianaki et al. (2008) studied building envelope airtightness by measuring air infiltration in 20 homes in Greece through two methods: tracer-gas leak testing and pressure testing. The air exchange rates in the buildings were measured at different pressures, and the results from the two methods were compared. Montoya et al. (2010) studied several homes under different conditions in Spain. Using the pressure test method, they calculated the air exchange rates for various building elements,

such as climate, materials, and number of floors. The data collected in the analytical and empirical research of [Chen et al. \(2012\)](#) provided a method for predicting the infiltration of pollutant particles through seal joints and openings. The leakage geometry and dimensions, air velocity in the leakage, and infiltration coefficient of pollutant particles with different dimensions were calculated. [Han et al. \(2015\)](#) reviewed the strategies for the numerical modeling of air infiltration rates by using EnergyPlus software in the United States. Their comparison of the experimental and numerical results of the models yielded infiltration rates of 2–11%.

Unwanted infiltration, which has been studied as an external parameter affecting the energy loads of buildings, has been found to be an important factor in energy consumption reduction ([Mattingly and Peters, 1977](#); [Anderlind, 1985](#); [Ren and Chen, 2015](#); [Happle et al., 2018](#)). In a recent study, [Goubran et al. \(2017\)](#) calculated the infiltration rate in glass entrance doors through simulations and experiments. They also studied the effects of infiltration on building energy consumption. [Younes et al. \(2012\)](#) evaluated air infiltration through walls. Infiltration was comprehensively investigated through simulations and other comprehensive evaluation and measurement techniques, as well as assessments of the interactions with other heat transfer factors. In addition, the effects of wind direction and degrees on façades and the impact of infiltration on wind energy in buildings were investigated because of their potential contribution to energy waste and excessive consumption. [Jurelionis and Bouris \(2016\)](#) applied computational fluid dynamics to the calculation of surface pressure distribution on building surfaces for three city models and two wind directions. Pressure differences and air change rates were derived in order to predict the heating load required to cover the heat loss caused by air infiltration. [Jokisalo et al. \(2009\)](#) studied the relationships among building envelope airtightness, infiltration, and energy use in a typical modern detached house in the cold Finnish climate. The influence of leakage distribution and wind and climate conditions on the infiltration rate and energy consumption was assessed. Infiltration was found to account for 15–30% of the energy used for space heating, including ventilation, in the typical Finnish detached house. Other studies have estimated that infiltration accounts for 25–50% of the heating load in residential and commercial buildings ([Kirkwood, 1977](#); [Nevrala and Etheridge, 1977](#)). [Persily \(1982\)](#) attributed one-third of the heating and cooling loads in a building to infiltration.

Thus, several studies have explored the methods for reducing infiltration and exfiltration and controlling energy loss in buildings. However, the influence of the exterior façade geometry on the infiltration rate resulting from wind pressure has not been addressed. Redesigning an exterior façade is simpler and less expensive than redesigning an entire building form. Improving the geometry of the exterior glass façade to control infiltration and energy consumption in existing construction, especially high-rise buildings, is possible.

2.1. Wind Pressure-Driven Infiltration

Infiltration airflow is driven by a pressure gradient across the building envelope. The driving pressure has two primary components: wind pressure and stack pressure. Mechanical air-moving systems also induce pressure differences across the envelope. The focus of this research was wind pressure, which is affected mainly by wind velocity, wind direction, local terrain and topography, and building shape characteristics ([Younes et al., 2012](#)). When the wind interacts with a façade, static pressure is distributed on the building's exterior surface. Wind pressure is generally positive with respect to the static pressure in the undisturbed airstream on the windward side of a building and negative on the leeward sides. The static pressure over building surfaces is almost proportional to the

velocity pressure of the undisturbed airstream (ASHRAE, 2009). Wind flows produce velocity and pressure fields on building envelopes. The relationship between the velocity and related pressure at different locations of the flow field can be obtained from Bernoulli's equation:

$$p_w = C_p \rho \frac{U^2}{2} \quad (1)$$

where p_w is the wind surface pressure relative to the outdoor static pressure in the undisturbed flow, ρ is the outside air density (kg/m^3), U is the velocity of the wind (m/s), and C_p is the wind surface pressure coefficient. The wind pressure coefficient C_p values depend on the building shape, wind direction, vegetation, terrain features, and influence of nearby buildings. The accurate determination of C_p can be obtained only from wind tunnel model tests of the specific site and building. The wind pressure distribution around a building is an important parameter in multizone airflow simulations. Current multizone air infiltration models generally deal with pressure coefficients as an input regardless of the technique used to provide the data. Because of natural wind, the pressure distribution around a building is affected by a number of variables. The wall-averaged values of C_p are usually estimated for multizone infiltration airflow calculation models. However, generating C_p values by numerical models based on parametrical analyses of wind tunnel test results is more accurate (Grosso, 1992). Surface-averaged pressure coefficients C_p can be used to determine the ventilation and infiltration rates. Figure 1 shows the pressure coefficient C_p averaged over entire wall of a low-rise building (Swami and Chandra, 1987).

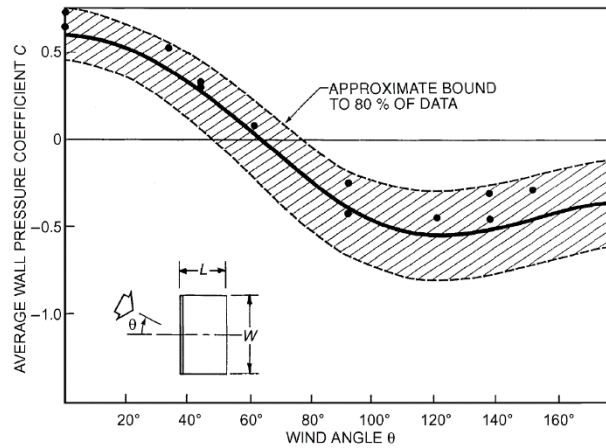


Figure 1 Variation of surface-averaged pressure coefficients for low-rise buildings (Swami and Chandra, 1987)

3. Methods

The aim of this study was to investigate the effects of building glass façade geometry on wind infiltration and the associated heating and cooling energy consumption. Even though air infiltration is a significant facet of building physics, its role is still unclear mostly because of measurement difficulties. Thus, the experimental database available for developing infiltration evaluation techniques and methods is limited. Another reason is the wide variety of construction techniques and practices, each of which is distinguished by multiple infiltration characteristics (Liddament, 1986).

In the present study, a building energy simulation was performed to evaluate the infiltration rates with regard to wind pressure and energy consumption in four models with different façade geometries. The forms of these façades were simple, indented, convex, and concave. The simulations were performed with DesignBuilder. This software uses

EnergyPlus, which was developed by the U.S. Department of Energy. To perform the simulations, four models with different air exchange rates caused by wind infiltration were simulated and analyzed in four Iranian cities with different climates and energy consumption patterns. The four cities were Yazd, Bandar Abbas, Tabriz, and Rasht. DesignBuilder is used in many of the research projects related to the effects of building geometries on indoor environments and energy consumption. It dynamically simulates the heating and cooling loads and the various types of energy used in buildings (Sailor, 2008; Yu et al., 2015).

Infiltration has long been recognized as a key component in heating and cooling loads. Several methods can account for infiltration in load calculations and facilitate more detailed energy analyses. The approaches in this energy simulation software were based on the relationships among the infiltration rates. The calculations considered multizone airflow models, weather conditions, and building characteristics, including envelope geometry and heating, ventilation, and air conditioning systems.

DesignBuilder software uses the following empirical equation (Achenbach and Coblenz, 1963) to calculate infiltration:

$$\text{Infiltration} = I_{\text{design}} F_{\text{schedule}} [A + B/|\Delta T| + C W_s + D W_s^2] \quad (2)$$

where I_{design} is defined by the software as the design infiltration rate (m^3/s), which is the airflow through the building façade under design conditions. F_{schedule} is a factor between 0 and 1 that can be scheduled to account for the effects of fan operation on infiltration, $|\Delta T|$ is the absolute indoor–outdoor temperature difference ($^{\circ}\text{C}$), and W_s is the wind speed (m/s). It should be noted that DesignBuilder varies the outdoor temperature and wind speed by zone height for the calculations. A , B , C , and D are constants, the values for which are suggested in the EnergyPlus user manual (Ng et al., 2014). These values are based on studies in low-rise buildings; thus, they might not be applicable to taller buildings and mechanically ventilated buildings.

3.1. Model Description

An attempt was made to reduce the variables. Thus, the energy savings related to cooling and heating energy consumption were limited to the variations in the wind infiltration associated with the façade geometries in each climate. The independent variables in the four simulated models (convex, concave, simple, and indented) are illustrated in Figures 2 and 3. The dimensions of the simulated single-building models were $D = 10 \text{ m}$, $W = 10 \text{ m}$, and $H = 12 \text{ m}$. There were no openings on the northern, eastern, and western exterior walls. The southern façade was glass. In accordance with the existing standards, the minimum temperature for heating was 21°C , and the maximum for cooling was 26°C . To calculate energy consumption in the software, an electric fuel cooling system with a coefficient of performance (COP) of 2.5 and a natural gas fuel heating system with COP of 1 were considered.

In the simulation, the presence of people and the use of lighting equipment and other devices in the space were not considered. The exterior walls and ceilings of the models were of materials with high thermal mass, with a homogeneous thermal insulation that had heat transfer coefficients of $0.5 \text{ W}/\text{m}^2 \text{ }^{\circ}\text{K}$ and $0.4 \text{ W}/\text{m}^2 \text{ }^{\circ}\text{K}$ for the base sample ceilings and walls, respectively. The color of the ceilings and the outer walls, which were exposed to direct sunlight, had an absorption coefficient of 60%. The southern façade was double-skin glass, with flat glass in the inner skin and different glass geometries in the outer skin. The transparent glass on the façade was double-glazed with a thermal break aluminum profile. The heat transfer coefficient, the shading coefficient, the visible light transmission coefficient, and the solar transmission coefficient of the glass were $2.67 \text{ W}/\text{m}^2 \text{ }^{\circ}\text{K}$, 0.76, 0.79,

and 0.61, respectively. In each model, the double-skin façade with a 0.04 m aluminum frame and six horizontal and vertical aluminum dividers was in a fixed position without inner or outer shading devices. The intermediate cavities of the four models were considered to be unconditioned because of the volume differences; thus, they were not included in the energy consumption calculations. It must be noted that in the energy consumption estimations, the variations in the solar gain from the southern façade were not considered for any of the models. Consequently, the differences in the results were limited to the wind-driven infiltration rates in each model and climate.

In the calculated models, wind direction and speed were considered to be fixed factors; thus, the infiltration results were limited to the geometry of the glass façade. The wind speed was considered in two modes at 5 and 10 m/s from the southern front and perpendicular to the models, respectively. The internal pressure coefficients of the models, the temperature differences between the interior and exterior, and the air density were considered to be -0.2 , 10°C , and 1.2 kg per cubic meter, respectively. Some factors, such as natural and mechanical ventilation and the stack effect, were ignored in the infiltration calculations and subsequent simulations; thus, the air exchange rate was limited to wind-driven infiltration.

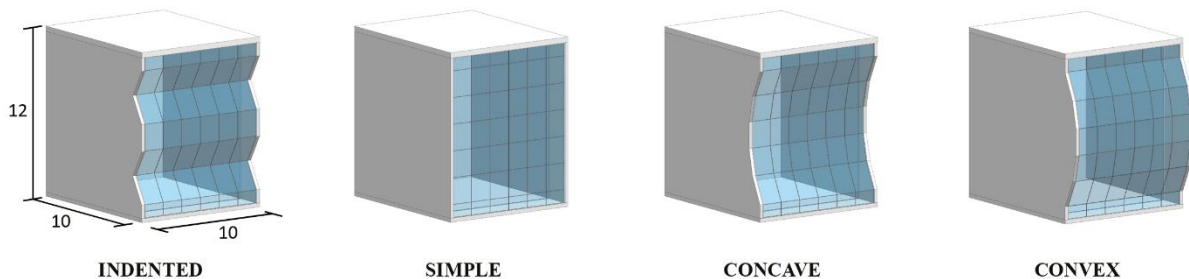


Figure 2 Three-dimensional simulations of the convex, concave, simple, and indented models

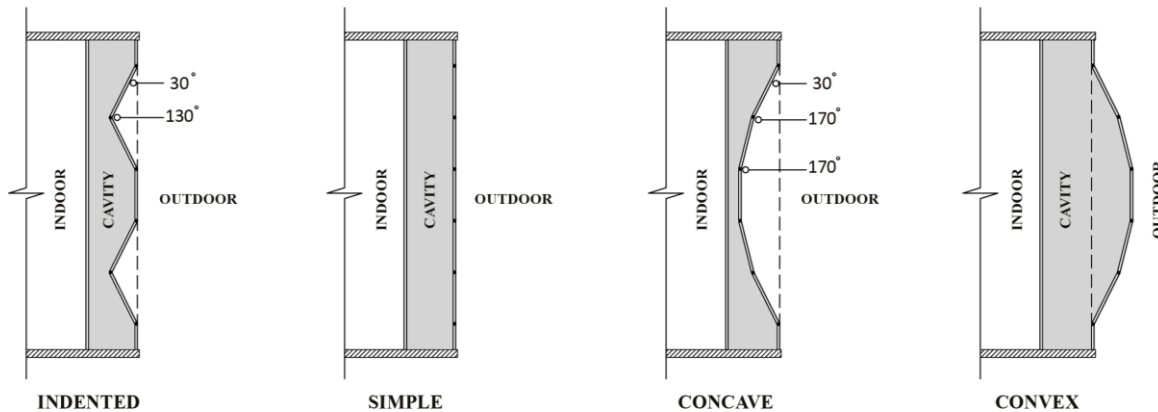


Figure 3 Cross-sections of the convex, concave, simple, and indented glass façades

3.2. Climate and Context

Four models with different air exchange rates caused by wind pressure-driven infiltration were simulated and analyzed in four Iranian cities with different climates and energy demands. The four cities were Yazd, Bandar Abbas, Tabriz, and Rasht. The main reason for choosing these cities was their different climatic conditions. Figure 4 shows their monthly average dry-bulb temperatures and relative humidity. According to the provided data and several climatic classifications, Yazd, Bandar Abbas, Tabriz, and Rasht are in the hot-arid, hot-humid, cold-arid, and moderate zones, respectively, in Iran. In this simulation, the hourly weather profiles of the cities were based on a typical meteorological

year. These data were extracted from the Iranian Meteorological Organization statistics that comprise hourly wet- and dry-bulb temperatures, dew points, relative humidity, cloud cover, wind direction, wind velocity, direct and diffuse solar radiation, and atmospheric pressure.

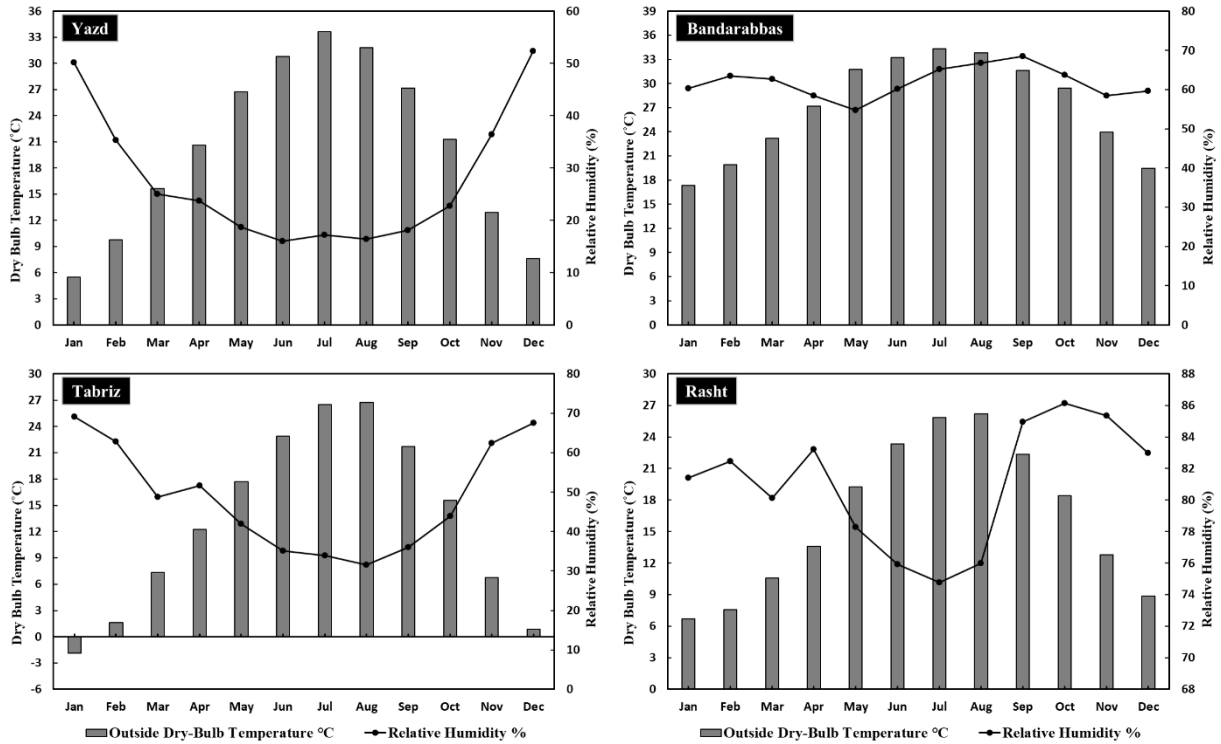


Figure 4 Monthly average dry-bulb temperatures and relative humidity in the Yazd, Bandar Abbas, Tabriz, and Rasht

4. Results and Discussion

The first part of the results provides the calculations of the indoor air exchange rates from wind infiltration at speeds of 5 and 10 m/s in the four models (Table 1). The purpose of this study was to investigate the wind-driven infiltration rate from the windward façades of buildings with different geometries. The changes in infiltration resulted from the differences in the wind pressure coefficients, and this was caused by the external wind pressure at the various geometries of the building façades. The wind pressure at the façade with convex geometry was transferred to the central point of the geometry, thus increasing the infiltration airflow rate by creating additional pressure in the central part of the façade. In this case, the nominal air exchange rate described the rate of the air infiltration in the building or zone. More wind pressure accumulated on the façades with indented geometry; thus, the wind infiltration rate in this geometry was higher than that in the other models. In contrast, the wind pressure and air infiltration rate were lower in the convex geometry model. The wind pressure was transferred to the exterior surfaces of the model, and the total wind pressure on the façades was reduced aerodynamically. The results indicated that in the convex model, the infiltration rate in air changes per hour was 0.36 lower than that in the indented model. These modes of air exchange can significantly affect energy consumption, air quality, indoor thermal comfort, weather conditions, building operation, and use. However, the effects of this parameter are climate-dependent.

Table 1 Calculations of wind infiltration-related internal air exchange rates at speeds of 5 and 10 m/s in four simulated models

Simulated model	Infiltration Air Change Rate per Hour (ACH)	
	5 m/s	10 m/s
Simple	2.3941	4.7881
Indented	2.4734	4.9469
Convex	2.2912	4.5825
Concave	2.4325	4.8651

The second part of the results represents the monthly heating and cooling energy consumption in the cities in four simulated models with infiltration air change rates of 10 m/s that were derived from the first part of the results. As was mentioned, for the energy calculations, the cooling and heating energy consumption resulting from the changes in wind infiltration in the interior spaces was investigated. The determination of the energy demands for the ventilation or lighting of the models was not the goal of this study. However, the geometry of a façade is an important influence on the amount of light and solar gain. The variations in the solar energy received from the glass façade were not considered in order to limit the heating or cooling energy consumption results to wind infiltration. The simulation results for Yazd city are illustrated in Figure 5. The lowest monthly cooling energy consumption was observed in the simulated convex model, and the highest, in the indented model. The maximum savings in cooling energy consumption in the convex model were 5.3% more than the indented model in May, June, and July. Similar to the case with cooling energy consumption, the monthly heating energy consumption in the convex and indented models was lower than that in the other models. The convex model yielded 7.2% more energy savings than the indented model in January. In addition, the energy savings in the warm months of the year were greater; 13% in May.

Figure 6 shows that the variations in the monthly heating and cooling energy consumption associated with the proposed profiles in Tabriz decreased over time. The maximum monthly energy savings from the convex model were 4.9% greater than the savings from the indented model in July. In addition, the maximum monthly energy savings from the convex model were 8.5% greater than the savings from the indented model in May and October.

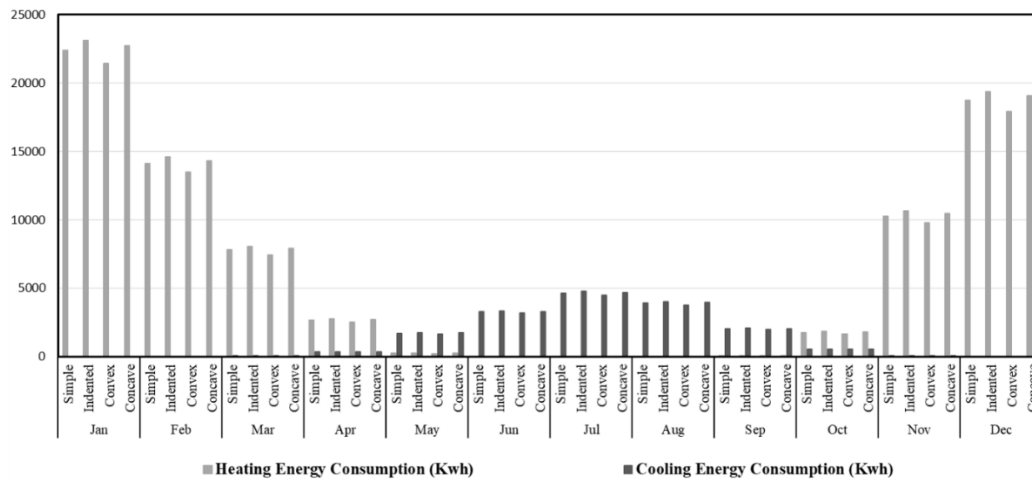


Figure 5 Heating and cooling energy consumption in the four simulated models in Yazd

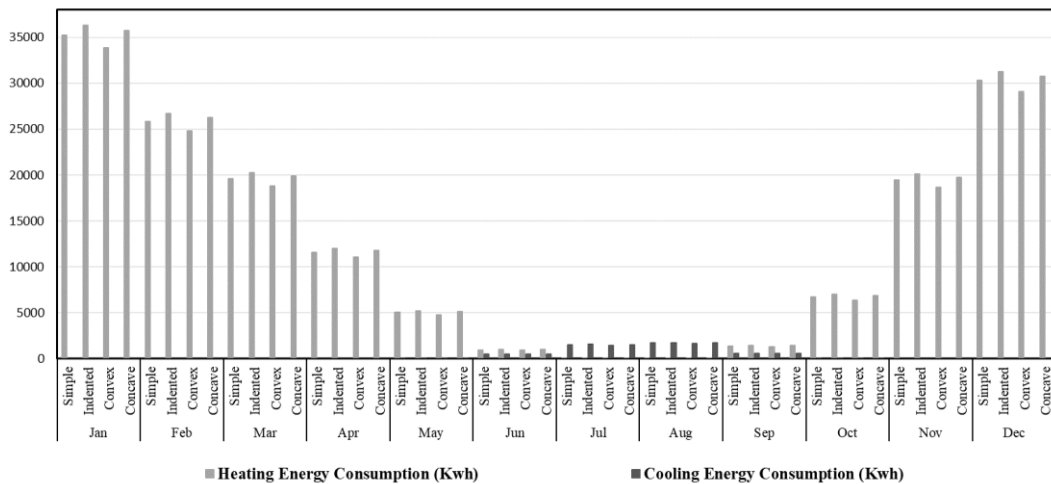


Figure 6 Heating and cooling energy consumption in the four simulated models in Tabriz

Figure 7, which relates to Rasht, shows that the monthly cooling energy consumption in the convex model was lower than that in the other simulated models. Thus, the maximum monthly energy savings in the convex model were greater than the savings (4.4%) yielded by the indented model in July. In addition, the convex model yielded 7% more energy savings than the indented model in January. In the warm months, the energy savings were greater: as much as 12% in September.

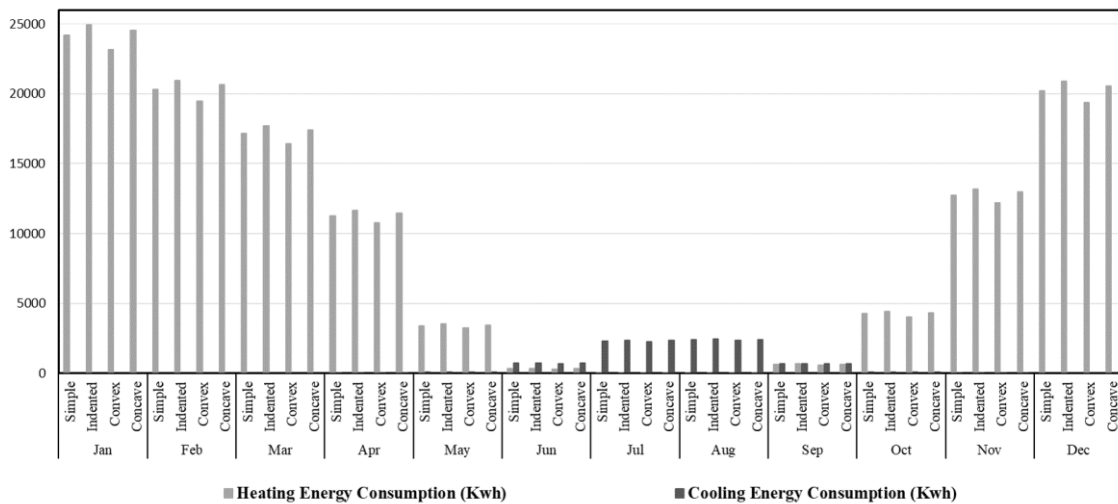


Figure 7 Heating and cooling energy consumption in the four simulated models in Rasht

Figure 8 shows the results of the study for Bandar Abbas. This city had the lowest monthly heating and cooling energy consumption for the convex model and the highest for the indented model. The monthly heating consumption varied for the four simulated Bandar Abbas models. The convex model yielded 8.6% more energy savings than the indented model in January. In the equinox, the savings increased: 14.4% in March and 16.6% in November. The maximum monthly energy savings for the convex model were 42% greater than those for the indented model in April. Moreover, the results for the monthly energy consumption in this city indicated that the highest cooling energy consumption in the convex model was 5.7%, more than that in the indented model from June to September.

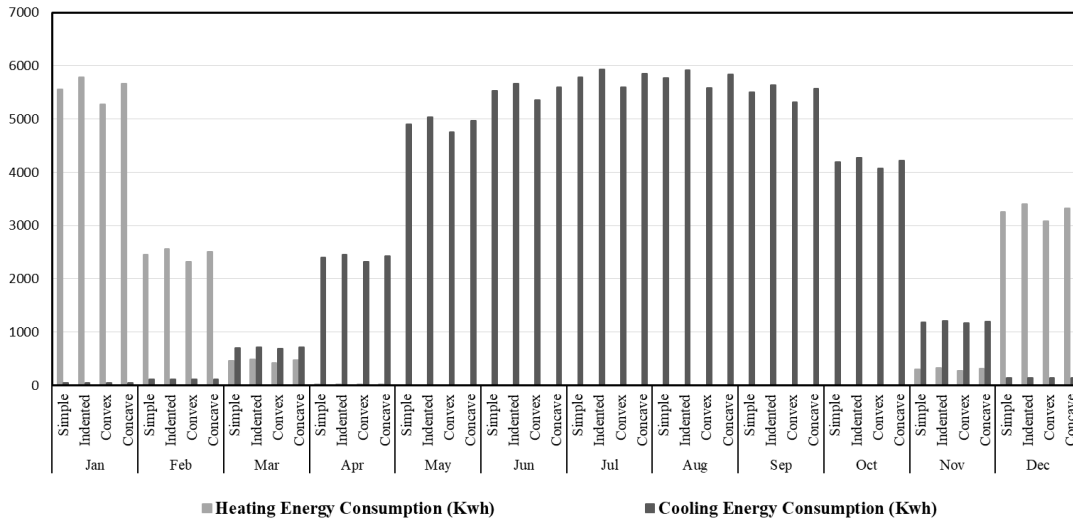


Figure 8 Heating and cooling energy consumption in the four simulated models in Bandar Abbas

The final part of the results addressed the total heating and cooling energy consumption for the four models in the cities under study. Figure 9 shows that the variations in energy consumption in each climate were based on the wind infiltration rates resulting from the façade geometries. The results indicated that in each city, the convex model had the lowest energy consumption, and the indented model had the highest. In the convex models, the annual cooling energy savings for Yazd, Tabriz, Rasht and Bandar Abbas were 5%, 4.3%, 3.7%, and 5.3% more than the savings in the indented models, respectively. The annual heating energy savings in the convex models were much greater than the savings in the indented models. The savings were 7.6% in Yazd, 7.1% in Tabriz, 7.3% in Rasht, and 9.5% in Bandar Abbas. These results highlight the previously discussed effects of air infiltration rates on heating energy consumption. Infiltration played a greater role in the heating and cooling energy savings in the convex geometry model in Bandar Abbas, which has a hot and humid climate, than in the other climates. The study also demonstrated the effects of unwanted wind infiltration on heating and cooling energy consumption in different climates. This was found to be related to the glass façade geometry of the models.

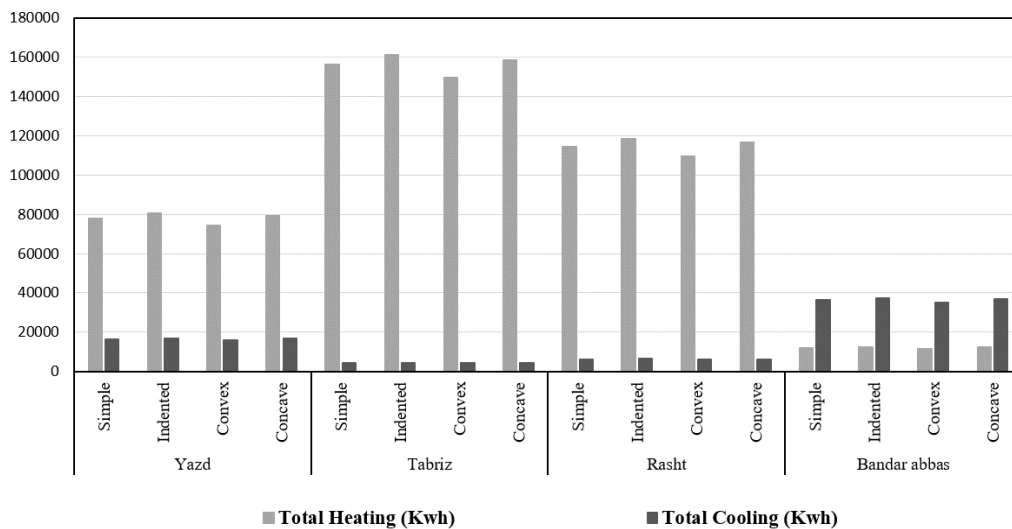


Figure 9 Annual heating and cooling energy consumption in the simulated models in the Yazd, Tabriz, Rasht and Bandar Abbas

5. Conclusions

Sustainable development principles in the built environment have encouraged researchers to focus on more efficient building envelopes. Façades, as a principal constituent of building envelopes, have a vital role in protecting indoor environments and controlling the interactions between outdoor and indoor spaces. The design and implementation of façade building systems can have positive effects on energy waste reduction and air leakage. Infiltration control through façade geometry plays an important role in building energy consumption. The purpose of this study was to investigate the effects of façade geometries on wind infiltration rates and heating and cooling energy consumption in buildings in four climates in Iran. Four models with convex, concave, simple, and indented geometries were simulated in Design Builder and studied in Yazd, Tabriz, Rasht, and Bandar Abbas, which are in the hot–arid, cold–arid, moderate, and hot–humid zones. The results confirmed that the interaction of the wind with the concave spaces in the double-skin façades with concave and indented geometry increased the wind pressure and air infiltration rates. In the convex model, the wind pressure and air infiltration rate were lower. The wind pressure was transferred to the exterior surfaces, and the total wind pressure on the exterior façade was reduced. In addition, the increase in the air infiltration rate increased cooling and heating energy consumption.

The results indicate that the energy consumption in the analyzed cities was lowest in the convex model and highest in the indented geometry model. The annual cooling energy savings in the convex models for the Yazd, Tabriz, Rasht, and Bandar Abbas were 5%, 4.3%, 3.7%, and 5.3% more than the savings in the indented models, respectively. In addition, the annual heating energy savings for the mentioned cities in the convex model were estimated as 7.6%, 7.1%, 7.3%, and 9.5% greater than the indented model. In general, the unwanted infiltration related to the façade geometry had a much greater effect on heating energy consumption than on cooling energy consumption. In addition, the façade geometry had a significant effect on heating and cooling energy consumption in the hot climates.

Four glass façade geometries were simulated in this study. Based on the results in the four climate regions, the designer must evaluate the available facilities and estimate the construction costs for the most appropriate geometry. Redesigning the glass façade is less costly, and it does not affect the interior spaces. Also, this method can be applied to existing buildings which reduces the need for mechanical heating or cooling systems and associated costs. Last, considering the quality of materials and their associated infiltration rates, designers can draft intelligent façades to increase the energy efficiency of new and existing buildings by adapting the geometries to account for wind pressure and direction.

References

- Achenbach, P., Coblenz, C., 1963. Field Measurements of Air Infiltration in Ten Electrically Heated Houses. *ASHRAE Transactions*, Volume 69, pp. 358–365
- Anderlind, G., 1985. Energy Consumption due to Air Infiltration. *In: Proceedings of the 3rd ASHRAE/DOE/BTECC Conference on Thermal Performance of the Exterior Envelopes of Buildings*
- ASHRAE. 1997. Handbook of Fundamentals. American Society of Heating, Refrigerating and Air-Conditioning Engineers, Atlanta
- ASHRAE. 2009. Handbook of Fundamentals. Chapter 16: Ventilation and Infiltration. USA Society of Heating, Refrigeration and Air-Conditioning Engineers, Atlanta

- Chen, C., Zhao, B., Zhou, W., Jiang, X., Tan, Z., 2012. A Methodology for Predicting Particle Penetration Factor Through Cracks of Windows and Doors for Actual Engineering Application. *Building and Environment*, Volume 47, pp. 339–348
- Ghaffarianhoseini, A., Ghaffarianhoseini, A., Berardi, U., Tookey, J., Li, D.H.W., Kariminia, S., 2016. Exploring the Advantages and Challenges of Double-Skin Façades (DSFs). *Renewable and Sustainable Energy Reviews*, Volume 60, pp. 1052–1065
- Goubran, S., Qi, D., Saleh, W.F., Wang, L.L., 2017. Comparing Methods of Modeling Air Infiltration through Building Entrances and Their Impact on Building Energy Simulations. *Energy and Buildings*, Volume 138, pp. 579–590
- Grosso, M., 1992. Wind Pressure Distribution around Buildings: A Parametrical Model. *Energy and Buildings*, Volume 18(2), pp. 101–131
- Han, G., Srebric, J., Enache-Pommer, E., 2015. Different Modeling Strategies of Infiltration Rates for an Office Building to Improve Accuracy of Building Energy Simulations. *Energy and Buildings*, Volume 86, pp. 288–295
- Happle, G., Fonseca, J.A., Schlueter, A., 2018. A Review on Occupant Behavior in Urban Building Energy Models. *Energy and Buildings*, Volume 174, pp. 276–292
- Hong, A.W.-T., Ibrahim, K., Loo, S.-C., 2019. Urging Green Retrofits of Building Façades in the Tropics: A Review and Research Agenda. *International Journal of Technology*, Volume 10(6), pp. 1140–1149
- Jackman, P., 1974. Heat Loss in Buildings as a Result of Infiltration. *Building Services Engineer*, Volume 42, pp. 6–15
- Ji, Y., Cook, M., Hunt, G., 2005. CFD Modelling of Buoyancy-Driven Natural Ventilation Opposed by Wind. In: Proceeding 9th International Building Performance Simulation Association Conference, Montreal, Canada, pp. 207–214
- Jokisalo, J., Kurnitski, J., Korpi, M., Kalamees, T., Vinha, J., 2009. Building Leakage, Infiltration, and Energy Performance Analyses for Finnish Detached Houses. *Building and Environment*, Volume 44(2), pp. 377–387
- Jurelionis, A., Bouris, D., 2016. Impact of Urban Morphology on Infiltration-Induced Building Energy Consumption. *Energies*, Volume 9(3), pp. 1–13
- Kirkwood, R., 1977. Fuel Consumption in Industrial Buildings. *Building Services Engineer*, Volume 45(3), pp. 23–31
- Liddament, M.W., 1986. *Air Infiltration Calculation Techniques: An Applications Guide*. Air Infiltration and Ventilation Centre, University of Warwick, Berkshire, United Kingdom
- Lstiburek, J., Pressnail, K., Timusk, J., 2002. Air Pressure and Building Envelopes. *Journal of Thermal Envelope and Building Science*, Volume 26(1), pp. 53–91
- Luo, Y., Zhang, L., Liu, Z., Wang, Y., Meng, F., Wu, J., 2016. Thermal Performance Evaluation of an Active Building Integrated Photovoltaic Thermoelectric Wall System. *Applied Energy*, Volume 177, pp. 25–39
- Mattingly, G.E., Peters, E.F., 1977. Wind and Trees: Air Infiltration Effects on Energy in Housing. *Journal of Wind Engineering and Industrial Aerodynamics*, Volume 2(1), pp. 1–19
- Montoya, M.I., Pastor, E., Carrie, F.R., Guyot, G., Planas, E., 2010. Air Leakage in Catalan Dwellings: Developing an Airtightness Model and Leakage Airflow Predictions. *Building and Environment*, Volume 45(6), pp. 1458–1469
- Nevrala, D., Etheridge, D., 1977. Natural Ventilation in Well-Insulated Houses. In: Proceedings of International Centre for Heat and Mass Transfer, International Seminar, UNESCO, Dubrovnik, Croatia
- Ng, L.C., Persily, A.K., Emmerich, S.J., 2014. Improving Infiltration in Energy Modeling. *ASHRAE Journal*, Volume 56(7), pp. 70–72

- Omer, A.M., 2008. Green Energies and the Environment. *Renewable and Sustainable Energy Reviews*, Volume 12(7), pp. 1789–1821
- Pacheco, R., Ordóñez, J., Martínez, G., 2012. Energy Efficient Design of Building: A Review. *Renewable and Sustainable Energy Reviews*, Volume 16(6), pp. 3559–3573
- Persily, A., 1982. *Understanding Air Infiltration in Homes, Report PU/CEES/= 129*. Princeton, NJ: Princeton University Center for Energy and Environmental Studies
- Powell, F., Krarti, M., Tuluca, A., 1989. Air Movement Influence on the Effective Thermal Resistance of Porous Insulations: A Literature Survey. *Journal of Thermal Insulation*, Volume 12(3), pp. 239–251
- Rantala, J., Leivo, V., 2009. Heat, Air, and Moisture Control in Slab-on-Ground Structures. *Journal of Building physics*, Volume 32(4), pp. 335–353
- Relander, T.-O., Thue, J.V., Gustavsen, A., 2008a. Air Tightness Performance of Different Sealing Methods for Windows in Wood-Frame Buildings. *In: Proceedings of the 8th Nordic Symposium on Building Physics, Copenhagen, Denmark*, pp. 417–424
- Relander, T.-O., Thue, J.V., Gustavsen, A., 2008b. The Influence of Different Sealing Methods of Window and Door Joints on the Total Air Leakage of Wood-Frame Buildings. *In: Proceedings of the 8th Nordic Symposium on Building Physics, Copenhagen, Denmark*, pp. 497–504
- Ren, Z., Chen, D., 2015. Simulation of Air Infiltration of Australian Housing and Its Impact on Energy Consumption. *Energy Procedia*, Volume 78, pp. 2717–2723
- Russ, N.M., Hanid, M., Ye, K.M., 2018. Literature Review on Green Cost Premium Elements of Sustainable Building Construction. *International Journal of Technology*, Volume 9(8), pp. 1715–1725
- Sailor, D.J., 2008. A Green Roof Model for Building Energy Simulation Programs. *Energy and Buildings*, Volume 40(8), pp. 1466–1478
- Sfakianaki, A., Pavlou, K., Santamouris, M., Livada, I., Assimakopoulos, M.-N., Mantas, P., Christakopoulos, A., 2008. Air Tightness Measurements of Residential Houses in Athens, Greece. *Building and Environment*, Volume 43(4), pp. 398–405
- Sherman, M.H., 1987. Estimation of Infiltration from Leakage and Climate Indicators. *Energy and Buildings*, Volume 10(1), pp. 81–86
- Swami, M., Chandra, S., 1987. Procedures for Calculating Natural Ventilation Airflow Rates in Buildings (No. FSEC-CR-163-86). Florida Solar Energy Center, Cape Canaveral, FL.
- Yin, R., Xu, P., Shen, P., 2012. Case Study: Energy Savings from Solar Window Film in Two Commercial Buildings in Shanghai. *Energy and Buildings*, Volume 45, pp. 132–140
- Younes, C., Shdid, C. A., Bitsuamlak, G., 2012. Air Infiltration Through Building Envelopes: A Review. *Journal of Building Physics*, Volume 35(3), pp. 267–302
- Yu, S., Cui, Y., Xu, X., Feng, G., 2015. Impact of Civil Envelope on Energy Consumption based on EnergyPlus. *Procedia Engineering*, Volume 121, pp. 1528–1534
- Yusuf, M.F., Ashari, H., Razalli, M.R., 2018. Environmental Technological Innovation and Its Contribution to Sustainable Development. *International Journal of Technology*, Volume 9(8), pp. 1569–1578